Vol.66: e23220245, 2023
https://doi.org/10.1590/1678-4324-2023220245
ISSN 1678-4324 Online Edition

Article - Engineering, Technology and Techniques

A Data-driven Robust Model for Day-ahead Operation Planning of Microgrids Considering Distributed Energy Resources and Demand Response

Mauro Obladen de Lara Filho[1]
https://orcid.org/0000-0002-7306-4369

Rafael Silva Pinto[1]
https://orcid.org/0000-0002-0574-1444

Cyntia Cristinne Corrêa Baia de Aquino[1]
https://orcid.org/0000-0002-5085-8086

Clodomiro Unsihuay-Vila[1]
https://orcid.org/0000-0002-1639-7765

Fabricio H. Tabarro[2]
https://orcid.org/0000-0002-0689-459X

[1]Universidade Federal do Paraná, Departamento de Engenharia Elétrica, Curitiba, Paraná, Brasil; [2]COPEL Distribuição, Departamento de Tecnologia e Qualidade dos Canais de Atendimento, Curitiba, Paraná, Brasil

Editor-in-Chief: Alexandre Rasi Aoki
Associate Editor: Alexandre Rasi Aoki

Received: 04-Apr-2022; Accepted: 22-Jul-2022

*Correspondence: mauroobladen4@gmail.com; Tel.: +55-41-996319861 (M.O.L.F.).

HIGHLIGHTS

- Novel data-driven approach to uncertainties in microgrid resources
- Faster convergence that stochastic optimization
- Reduced conservativeness compared to robust optimization
- Microgrid system with comprehensive selection of distributed energy resources

Abstract: The optimization of microgrids present challenges such as managing distributed energy resources (DERs) and the high reliance on intermittent generation such as PV and wind turbines, which present an aleatory behavior. The most popular techniques to deal with the uncertainties are stochastic optimization, which comes with a high computational burden, and adaptive robust optimization (ARO), which is often criticized for the conservativeness of its solutions. In response to these drawbacks, this work proposes a mixed-integer linear programming (MILP) model using a data-driven robust optimization approach (DDRO) solved by a two-stage decomposition using the column-and-constraint generation algorithm (C&CG). The DDRO model uses historic data to create the bounds of its uncertainty set, eliminating the conservativeness created by the arbitrary definition of the uncertainty set that is seen in ARO while maintaining a low computational burden. The DDRO model applied was not previously utilized in MGs, only in bulk power

systems. A benchmark MG system was simulated for a 24-hour period without uncertainties, with uncertainties using ARO (15% uncertainty budget) and with uncertainties and DDRO. The operational costs without uncertainty were $124,600,60, while the ARO approach rose those costs by 32.5% ($ 165,137.18). Finally, the DDRO approach managed to keep the costs in $ 126,934.54, a mere 1.8% increase from the base case without uncertainty. All simulations were performed in less than 1 minute. The results confirm a) the advantages of bounding the uncertainty set with historical data instead of an arbitrary definition of bounds and b) the fast-converging times of DDRO.

Keywords: Operation Planning; Microgrids; Data-Driven Robust Optimization; Demand Response; Distributed Energy Resources.

INTRODUCTION

Modern distribution systems have been steadily evolving from classic networks, where energy is generated in large plants outside the main consumption centers, to active distribution networks (ADNs), where the centralized generation is combined with the distributed generation from DERs, such as distributed generation (DG), energy storage systems (ESSs), and electric vehicles (EVs). These networks form a much more complex grid with bidirectional power flow, both from the larger grid to the consumers and from the consumers to the grid.

In this context, the microgrid (MG) concept emerged. A microgrid is a small-scale ADN that is composed of a group of DERs that can be managed by the same operator, aiming to maximize financial benefits, service reliability, and a variety of other objectives. Therefore, the rise in microgrid systems has stimulated the development of several optimization frameworks for microgrid operation in the literature. On the other hand, the number of possibilities to be considered in MG systems, regarding the different types of DERs, the optimization techniques, the objectives to be accomplished, and the topology of the system is enormous, guaranteeing that the subject still has plenty of opportunities for further development.

Regarding the topology of MGs, several works, such as (1–7) represent the network in a single-bus topology, which simplifies the optimization problem but makes the model unable to account for bus voltage and line power flow constraints. On the other side of the spectrum, some works, including (8–10), consider the most accurate network models with non-linear constraints that heavily increase the complexity and computational burden of the model. Finally, some works, such as (11–16) consider multiple-bus systems with linearized constraints to reduce complexity while maintaining important network aspects such as voltage control and line power flow constraints.

With the improvements in control technology in smart grids, demand response programs became feasible, especially demand side management (DSM). These programs are divided into price-based DSM, where hourly energy tariffs incentivize consumers to shift the operation of loads to less expensive periods, such as in (1), or incentive-based DSM, where financial incentives are directly offered to consumers to shift or curtail non-essential loads.

One of the most important factors to be considered in microgrid optimization is the fact that most MGs rely heavily on renewable generation, such as photovoltaic (PV) and wind turbines and the availability of these sources is dependent on weather conditions. Therefore, these sources have an intermittent and aleatory behavior in the short-term, leading to a significant amount of uncertainty in operation planning decisions. Also, load demand can suffer fluctuations from the average tendency in a short period of analysis. Despite that, many works in MG optimization, such as (1,3,8–11,17,18), and disregard uncertainties, which can bring problems to the MG operator if the weather conditions are different than forecasted.

Different techniques can be applied to cope with uncertain behavior. The work in (19) proposes a deterministic approach combined with a real-time algorithm to respond to uncertainty realization. Stochastic programming uses probability distribution functions to model the behavior of uncertain variables, generating scenarios that are weighted by their probability and thus obtaining an average operational condition, as can be seen in (2,4,12,14) . Even if stochastic optimization provides a thorough analysis considering a broad spectrum of possibilities, obtaining probability distribution functions for real-world variables is not straightforward and can be challenging. Also, the computational burden of generating thousands of scenarios can be high.

To solve the problem of obtaining probability distribution functions, work (13) utilizes adaptive robust optimization (ARO). ARO adopts a worst-case scenario approach, obtaining the worst possible realization in an interval-based uncertainty set, usually a polyhedric set. This approach eliminates the need for detailed knowledge of the probabilistic behavior of the uncertain variables and eases the computational burden,

obtaining a safe but often overly conservative result because the worst-case scenario of an uncertainty set that was defined without adequate historical data or probability functions can be far greater than the actual uncertainty of the variable.

To establish a compromise between the high computational burden of stochastic programming and the conservativeness of ARO, data-driven robust optimization (DDRO) offers an interesting option: it combines the robust optimization approach of optimizing for the worst-case scenario, eliminating the need for considering lots of scenarios and probability distributions and reducing the computational burden when compared to stochastic optimization, while providing a less conservative approach than ARO. In ARO, an arbitrary amount of uncertainty is considered for the uncertain variables via an uncertainty budget. This makes ARO solutions tend to be overly-conservative. In DDRO, historical data is used to create the bounds of the uncertainty set, providing more realistic and less conservative uncertainty sets.

In (15), historical data of uncertain variables are used as the uncertainty set. Therefore, the uncertain variable can assume values that have previously happened or a linear combination of historical scenarios, making the uncertainty set much closer to real-world behaviors than an arbitrarily defined budget-constrained set that can cause ARO based models to be extremely conservative, including scenarios with extremely low probability. This work, although not focused on MGs, but in traditional networks, offers an interesting possibility for works in the MG field. In (16), historical data is also used, but in a different approach compared to stochastic programming, called distributionally DDRO, where the past scenarios are used to estimate an empirical probability distribution function that is utilized to perform stochastic optimization.

In this work, the DDRO method considered is close to that of (15), where the uncertainty set is the convex hull of a set of points representing historical scenarios, eliminating the need of generating probability distributions as is done in distributionally DDRO and stochastic programming.

Considering the literature review, we propose a MG operational planning optimization model that includes:

- A data-driven robust optimization approach to uncertainties in load demand and photovoltaic generation
- A linearized network topology that is suitable for both radial and meshed microgrids and provides the possibility to consider voltage control and power flow constraints.
- Modelling of Battery Energy Storage Systems (BESSs), including degradation costs.
- Modelling of both non-dispatchable and dispatchable generation.
- A price-based demand response program
- A fast-converging column and constraint generation (C&CG) solving algorithm.

The novelty of this work is the application of a novel DDRO methodology that has not been utilized previously in a MG system, only in bulk power systems that lack the amount of DERs and other constraints that are present in MG systems, filling the research gap between stochastic optimization, that comes with a high computational burden, and ARO, which is often criticized by its conservativeness. We also highlight that most works found in the literature fail to consider at least one of the DERs considered in this work (ESS, demand response, dispatchable and non-dispatchable generation) while this work presents a detailed formulation of all these resources, including ESS degradation costs, price-based demand response, PV, and thermal generation.

MATERIAL AND METHODS

Proposed Model

The proposed model seeks to minimize the total operational costs of the MG in a 24-hour timespan for the worst possible uncertainty realization. These costs include the cost of exchanging energy from the upstream grid, the operational costs of the dispatchable generation, the cost of load shedding and the cost associated with battery degradation. Uncertainty is proposed in the PV generation and the load demand and formulated in a DDRO approach.

The objective function is represented in Equation (1).

$$\min_{x} \max_{y} \min_{u} TCost \tag{1}$$

In equation (1), x represents all the variables related to BESS, controllable loads, and the dispatchable generation, y represents the uncertain variables related to non-controllable loads and availability of PV generation, while u represents non-utilized PV generation.

The total cost ($TCost$) is composed of the cost of exchanging energy with the grid, the degradation cost of the batteries, the operational costs of dispatchable generators, and load shedding costs, as can be seen in (2).

$$TCost = \sum_{t=1}^{N} [\Delta t(C_t^{Grid} + C_t^{BESS} + C_t^{Dg})] + C^{LS} \quad (2)$$

The cost of exchanging energy with the upstream grid can be a positive value in case the MG is in an energy deficit and therefore purchasing energy from the grid, or a negative value, in case the MG is in an energy surplus situation and selling energy to the grid. Each bus of the MG has a net energy deficit or surplus in each period, that can be calculated as in (3).

$$NE_{t,b} = \Delta t(L_{t,b} + St_{t,b} - Gpv_{t,b} - Gdg_{t,b}) \quad (3)$$

where $NE_{t,b}$ represents the net energy surplus/deficit for bus b in period t, $L_{t,b}$ represents total load (controllable and non-controllable) in the bus for period t, $St_{t,b}$represents net BESS storage/discharge (positive values indicate the battery is charging in period t and negative values indicate discharge), $Gpv_{t,b}$ represents PV generation, and $Gdg_{t,b}$represents dispatchable generation.

Then, the net energy surplus/deficit of each bus is aggregated for all buses, representing the total surplus/deficit of the entire MG for a period t. This aggregated net energy is the value that must be purchased from the grid in a deficit situation or sold to the grid in a surplus situation. Thus, grid exchanging costs can be calculated as in (4).

$$C_t^{Grid} = \sum_{b=1}^{nb} NE_{t,b} * ET_t \quad (4)$$

where ET_t represents the energy tariff for period t.

BESS costs (C_t^{BESS}) are related to the battery degradation caused by cycling the battery. This degradation is mostly dependent on the depth of discharge (DoD) applied to the battery in a discharge cycle. A percentual degradation corresponds to each amount of DoD applied to the battery. The cost of this percentual degradation can be calculated by associating the degradation with the investment cost of purchasing the BESS, as in (5).

$$C_t^{BESS} = \sum_{b=1}^{nb} DEG_{t,b} * INV_b \quad (5)$$

where $DEG_{t,b}$represents percentual degradation caused by the discharge cycle applied in period t to a battery installed in bus b and INV_brepresents the investment cost of purchasing the battery in bus b. Further details on calculating $DEG_{t,b}$ are provided in section 2.2.

The cost of the dispatchable generation is represented in a linear function, with a fixed cost for committing the generator in period t and a variable cost that depends on the amount of power required, as can be seen in (6).

$$C_t^{Dg} = \sum_{b=1}^{nb} \Delta t * (A_b * Xdg_{t,b} + B_b * Gdg_{t,b}) \quad (6)$$

where A_b is the cost in $ associated with committing the generator in bus b, $Xdg_{t,b}$ is a binary variable that indicates if the generator in bus b has been committed in period t, B_b is the linear cost associated with the power dispatched from the generator.

Finally, load shedding costs apply if, for any reason, it is impossible to allocate all the controllable load in the 24-hour period, as in (7).

$$C^{LS} = \sum_{b=1}^{nb} LS_b * LST \quad (7)$$

where LS_b represents the total amount of load that was curtailed from bus b in the 24-hour timespan and LST represents the penalty costs associated with load shedding.

Equations (8) – (14) represent the operational constraints of the battery system.

$$X_{t,b}^{C} + X_{t,b}^{D} \leq 1 \tag{8}$$

$$X_{t,b}^{D} - X_{t-1,b}^{D} = Z_{t,b}^{ON} - Z_{t,b}^{OFF} \tag{9}$$

$$SoC_{t,b}^{MIN} \leq SoC_{t,b} \leq SoC_{t,b}^{MAX} \tag{10}$$

$$SoC_{t,b} = SoC_{t-1,b} + \Delta t * (St_{t,b}^{C} * \eta^{C} - \frac{St_{t,b}^{D}}{\eta^{D}}) \tag{11}$$

$$St_{t,b} = St_{t,b}^{C} - St_{t,b}^{D} \tag{12}$$

$$0 \leq St_{t,b}^{C} \leq St_{t,b}^{MAX} * X_{t,b}^{C} \tag{13}$$

$$0 \leq St_{t,b}^{D} \leq St_{t,b}^{MAX} * X_{t,b}^{D} \tag{14}$$

$X_{t,b}^{C}$ and $X_{t,b}^{D}$ are binary variables that indicate if the battery from bus b is charging (C) or discharging (D) in period t. Therefore, equation (8) guarantees that the battery cannot charge and discharge simultaneously. $Z_{t,b}^{ON}$ and $Z_{t,b}^{OFF}$ are binary variables that indicate the beginning and end of a discharge cycle according to equation (9), which is important to calculate degradation. Equation (10) establishes the state of charge (SoC) limits for each battery and (11) corresponds to the inter-temporal power balance in the battery system. Equation (12) calculates the net storage value from the battery installed in bus b in a period t and (13) and (14) limit the power of charge/discharge of the battery and guarantee that the battery will only be operated if the corresponding binary variable is activated.

Regarding battery degradation, the work in (20) presents a model for the degradation behavior of li-ion batteries, which is a non-linear exponential curve that correlates the DoD applied to the battery in each cycle and the percentual degradation. Since this work proposes a MILP model, that behavior had to be linearized using a piecewise linearization technique, where several linear functions are approximated to sections of the original non-linear curve and then, constraint (15) is applied to each of the linear functions.

$$DEG_b \geq LC_f + AC_f * DoD_b \quad \forall f \tag{15}$$

where LC_f and AC_f are the linear and angular coefficients of the linear function f among the linear functions that were approximated to the degradation curve. Equation (15) guarantees that the value of DEG_b is above that of the approximation, but since a higher value of DEG_b means a higher degradation cost for the battery, the solver will seek the lowest possible values, without violating (15).

The total load in the MG is divided into controllable and non-controllable loads. Non-controllable loads are forecasted on an hourly basis and uncertainty is applied, but controllable loads are provided on a per-bus basis. Each bus of the MG has an amount of controllable load to be allocated in any period of the day, and a percentage of that amount is allocated in each period, as in (16).

$$CL_{t,b}^{al} = dr_{t,b} * CL_b \tag{16}$$

where $CL_{t,b}^{al}$ represents the amount of controllable load allocated in bus b in period t, CL_b represents the total amount of controllable load to be allocated in bus b in the 24-hour timespan, and $dr_{t,b}$ represents the percentage of the total controllable load for bus b that has been allocated in period t. Equation (17) guarantees that the values of $dr_{t,b}$ are between 0 and 100% and (18) establishes that no more than 100% of the total controllable load for bus b is allocated in the 24-hour period.

$$0 \leq dr_{t,b} \leq 1 \tag{17}$$

$$\sum_{t=1}^{N} dr_{t,b} \leq 1 \tag{18}$$

Finally, if the sum of $dr_{t,b}$for the 24-hour period is smaller than 100%, it means that some portion of the controllable load for bus b has not been allocated, meaning it was curtailed. Then, the load shedding amount can be calculated from (19).

$$LS_b = \left(1 - \sum_{t=1}^{N} DR_{t,b}\right) * CL_b \tag{19}$$

Total load for a bus b in period t, required to calculate the net energy from equation (3), can be calculated as in (20).

$$L_{t,b} = CL_{t,b}^{al} + NCL_{t,b} \tag{20}$$

where $NCL_{t,b}$ represents non-controllable load.

The work in (21) presents a comprehensive formulation of thermal generators, considering ramp constraints and start-up and shut-down ramp constraints. In this work, for the sake of simplicity, the modelling of thermal generators is a simplified version of (21) where start-up and shut-down ramp rates are equal to the ramp rate for an already powered up generator, meaning there are no special constraints for the start-up and shut-down moments. Binary variable $Xth_{t,b}$ is activated when the thermal unit from bus b is committed in a period t, while binary variables $Yth_{t,b}$ and $Zth_{t,b}$ are activated if the thermal unit in bus b is starting up/shutting down in period t, respectively.

Equations (21)-(30) represent the thermal generation constraints. Further clarification can be found in (21).

$$Yth_{t,b} - Zth_{t,b} = Xth_{t,b} - Xth_{t-1,b} \tag{21}$$

$$Pdg_{t,b} \geq P_b^{min}\left(Xth_{t,b} - Zth_{t+1,b} - Yth_{t,b}\right) \tag{22}$$

$$Pdg_{t,b} \leq P_b^{max}\left(Xth_{t,b} - Yth_{t,b}\right) + R_b * Yth_{t,b} \tag{23}$$

$$Pdg_{t,b} \leq P_b^{max}\left(Xth_{t,b} - Zth_{t+1,b}\right) + R_b * Zth_{t+1,b} \tag{24}$$

$$Pdg_{t,b} - Pdg_{t-1,b} \leq P_b^{max} * Yth_{t,b} + R_b * (Xth_{t,b} - Yth_{t,} \tag{25}$$

$$Pdg_{t-1,b} - Pdg_{t,b} - \leq P_b^{max} * Zth_{t,b} + R_b * (Xth_{t,b} - Zth \tag{26}$$

$$Xth_{t,b} \geq Yth_{t,b} \tag{27}$$

$$Xth_{t,b} \geq Zth_{t-1,b} \tag{28}$$

$$Yth_{t,b} + Zth_{t,b} + Zth_{t+1,b} \leq 1 \tag{29}$$

$$Gdg_{t,b} = \Delta t * \frac{(Pdg_{t,b} + Pdg_{t-1,b})}{2} \tag{30}$$

Equations (21) and (27)-(29) establish the connections between binary variables. Equations (22)-(24) establish the minimum and maximum power output of the thermal generators according to the different stages of operations (start-up, shut-down, and normal operation). Equations (25)-(26) establish the ramp constraints for the same stages. Equation (30) calculates the energy delivery in each period.

In this work, a linearized power flow model based on (22) is utilized. This model has the advantages of being capable of representing voltage and power flow constraints for both radial and meshed networks. Equations (31)-(38) represent the constraints associated with the power flow model.

$$Pfl_{t,l} = A * (Va_t - Vb_t) + B * (\theta a_t - \theta b_t) \tag{31}$$

$$Qfl_{t,l} = B * (Va_t - Vb_t) + A * (\theta a_t - \theta b_t) \quad (32)$$

$$A = \frac{r_{ab}}{r_{ab}^2 + x_{ab}^2} \qquad B = \frac{x_{ab}}{r_{ab}^2 + x_{ab}^2} \quad (33)$$

$$-Pfl_l^{MAX} \leq Pfl_{t,l} \leq Pfl_l^{MAX} \quad (34)$$

$$-Qfl_l^{MAX} \leq Qfl_{t,l} \leq Qfl_l^{MAX} \quad (35)$$

$$\frac{NE_{t,b}}{\Delta t} - \sum_{l=1}^{\Omega b} Pfl_{t,l} = 0 \quad (36)$$

$$pf * \frac{NE_{t,b}}{\Delta t} - \sum_{l=1}^{\Omega b} Qfl_{t,l} = 0 \quad (37)$$

$$V^{MIN} \leq V_{t,b} \leq V^{MAX} \quad (38)$$

where r_{ab} and x_{ab} are the resistance and reactance from a feeder that connects buses a and b, Va_t and Vb_t are the voltages from buses a and b connected by feeder l in a period t and θa_t and θb_t are the angles associated with the same buses.

Equations (31)-(33) calculate active and reactive power flow in each feeder l and each period t, while (34) and (35) establish the maximum power flow value for each feeder. (36) establishes the power balance for each bus in the MG and (37) proposes a fixed power factor for all the MG, for the sake of simplicity. Finally, (38) establishes voltage limits for each bus of the system.

Considering on-grid operation of the MGs, peaks in energy demand from the upstream grid may be a challenge for the DSO and represent stability concerns for the grid and, therefore, should be avoided.

This concept can be illustrated by the load factor (LF), which is the ratio between the average power demand and the peak power demand of the MG, as in (39). A high LF means that the peak power of the system is not far greater than the average power demand, therefore, the operation is smooth and regular. A low LF means that the peak power is far greater than the average, which is undesirable.

To provide minimal impact on the upstream grid, it is proposed that the load factor of the MG after the optimization of DERs is not diminished harshly from the original value considering only the total load of the system. It is proposed that the new LF is limited to being above 80% of the original LF, as in constraint (40).

$$LF = \frac{\sum_{t=1}^{N} \sum_{b=1}^{nb} L_{t,b}}{24 * \max L_{t,b}} \quad (39)$$

$$\sum_{b=1}^{nb} NE_{t,b} \leq \frac{\sum_{b=1}^{nb} \sum_{t=1}^{N} NE_{t,b}}{24 * 0.8 * LF} \quad (40)$$

Delivery of power from PV generators depends on the available generation and on the operational conditions of the MG that may demand a curtailment of the PV generation to satisfy constraints. Equations (41) and (42) model this behavior.

$$Gpv_{t,b} = Gpv_{t,b}^{Av} - Gpv_{t,b}^{curt} \quad (41)$$

$$0 \leq Gpv_{t,b}^{curt} \leq Gpv_{t,b}^{Av} \quad (42)$$

where $Gpv_{t,b}^{Av}$ is the available PV generation for the PV system on bus b on period t and $Gpv_{t,b}^{curt}$ is the amount of PV generation that has been curtailed.

Solution Algorithm and Data-Driven Uncertainty Set

As stated in the previous section, the objective function of the problem is a tri-level min-max-min problem. The solution to this sort of problem is not trivial and cannot be handled by commercial solvers directly. Thus, it is necessary to decompose the problem in stages that can be resolved separately and aggregated further. Most robust optimization problems, such as (13,15), utilize the column and constraint generation (C&CG) algorithm, as shown in Fig. 1.

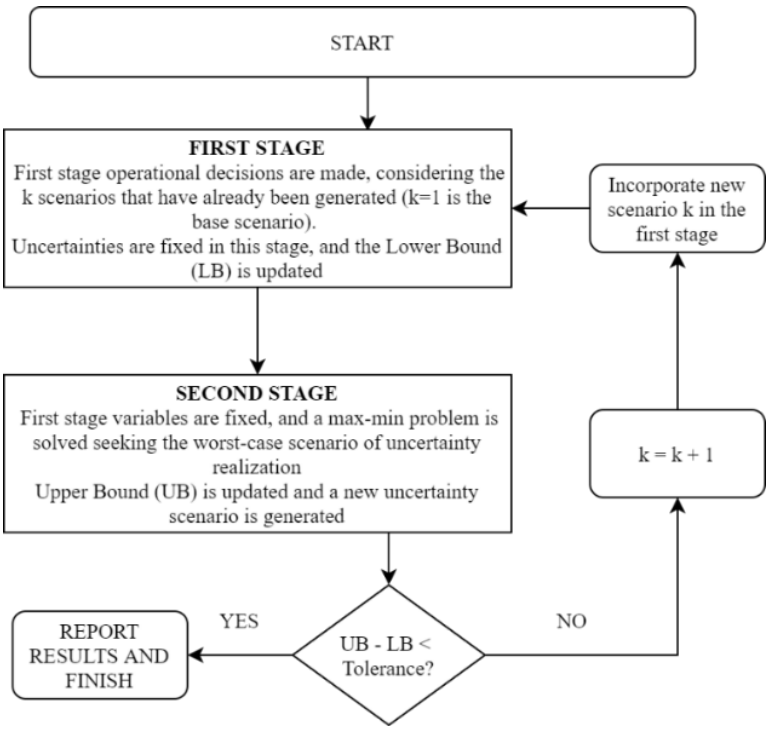

Figure 1. C&CG algorithm

In this formulation, the problem is divided into two stages. The first stage is a min problem where the operational decisions are initially made based on the forecasted scenario, without any uncertainties. In this stage, the availability of PV generation (Gpv^{Av}) and the non-controllable loads (NCL) are considered fixed parameters and the operational decisions regarding BESS, thermal generation and controllable loads are made.

After the solution of the first stage, the operational decisions are fixed in the second stage, and the constraints associated with these decisions are disregarded. Then, the availability of PV generation and the non-controllable loads, that are considered fixed parameters in the first stage, are now considered as variables, where the algorithm seeks the worst-case scenario of the uncertain variables for the operational decisions made in the first stag, bounding these variables to the data-driven uncertainty set.

The data-driven uncertainty set for PV availability is represented by equation (43), and the uncertainty set for non-controllable loads is represented in (44). Additional references for this formulation can be found in (15).

$$\boldsymbol{Gpv_b^{Av}} = \left\{\boldsymbol{Gpv_b^{Av}} \in R^{N\,x\,nb} \middle| \boldsymbol{Gpv_b^{Av}} = \sum_{d1=1}^{D1} \alpha g_{d1}\, \overline{\boldsymbol{Gpv_{b,d1}^{Av}}}, \sum_{d1=1}^{D1} \alpha g_{d1} = 1, \alpha g_{d1} \geq 0\right\} \tag{43}$$

$$\boldsymbol{NCL_b} = \{\boldsymbol{NCL_b} \in R^{N\,x\,b} | \boldsymbol{NCL_b} = \sum_{d2=1}^{D2} \alpha l_{d2}\, \overline{\boldsymbol{NCL_{b,d2}}}, \sum_{d1=1}^{D2} \alpha l_{d2} = 1, \alpha l_{d2} \geq 0\} \tag{44}$$

The uncertainty set is composed of D1 scenarios in case of PV, represented by $\overline{\boldsymbol{Gpv_{b,d1}^{Av}}}$ and D2 scenarios in case of NCL, represented by $\boldsymbol{NCL_{b,d2}}$. Each scenario represents one historical scenario (a full 24-hour period) that occurred in the past for each bus b. Therefore, the resulting scenario will be a linear combination

of the past scenarios, and the solver is responsible to find a combination of the weights $\alpha g_{d1}$and αl_{d2} that result in the worst-case scenario for the optimization process.

That creates a new scenario of the uncertain variables, which is then incorporated to the first level, and the optimization is conducted again, but with the addition of the new scenario generated in the second stage of the previous iteration. The process then continues until the objective functions present the same value in both the first and second stages. That means that the first stage could not reach a new solution that improved the objective function, nor the second stage could find an even worse scenario, meaning that this solution is the best solution for the worst-case scenario.

Simulation Results

All numeric experiments are carried out using Gurobi Optimizer in an Intel® Core® i5-7300HQ CPU with 8 GB of RAM. The formulation was made in Python language, using the Pyomo framework to connect Python and Gurobi.

The work in (23) presents a detailed benchmark test system for networked microgrids. In this work, 4 different MG systems are proposed, between radial and meshed topologies, including PV and wind generation as well as thermal units and one year of historical data for load demand and PV availability, which is crucial for the implementation of the DDRO model. Therefore, the MG system that is simulated in this work is adapted from (23), with a few differences, such as replacing wind turbines with PV generation, since PV provides additional challenges due to the unavailability of PV generation at night and in peak tariff hours, and disregarding the connections with the other MGs proposed, only considering the connection with the upstream grid. Line data (resistance and reactance) can be obtained in (23). Battery acquisition costs were considered to be $100/kWh. For all the test systems, the values are considered in per unit values (pu), with an 11 kV base voltage and 10 MVA base power.

The base scenario of the uncertain variables is taken from a random summer day among the one-year scenarios proposed in (23). The energy tariffs follow the Brazilian white tariff. The data associated with the chosen scenario can be seen in Table 1.

Table 1. Data for simulation

	Data		
Period	**% of peak load**	**% of peak PV**	**Energy Tariff ($/kWh)**
0-1AM	81	0	0.68559
1-2	77	0	0.68559
2-3	80	0	0.68559
3-4	79	0	0.68559
4-5	79	11	0.68559
5-6	82	20	0.68559
6-7	84	40	0.68559
7-8	87	60	0.68559
8-9	90	86	0.68559
9-10	94	100	0.68559
10-11	95	100	0.68559
11-12PM	94	100	0.68559
12-1	93	83	0.68559
1-2	91	56	0.68559
2-3	88	32	0.68559
3-4	87	23	0.68559
4-5	91	0	0.68559
5-6	95	0	0.93679
6-7	98	0	1.45488
7-8	100	0	1.45488
8-9	97	0	1.45488
9-10	94	0	0.93679
10-11	84	0	0.68559
11-12	88	0	0.68559

The microgrid considered for simulation has 6 buses and 11 lines, in a meshed topology shown in Figure 2.

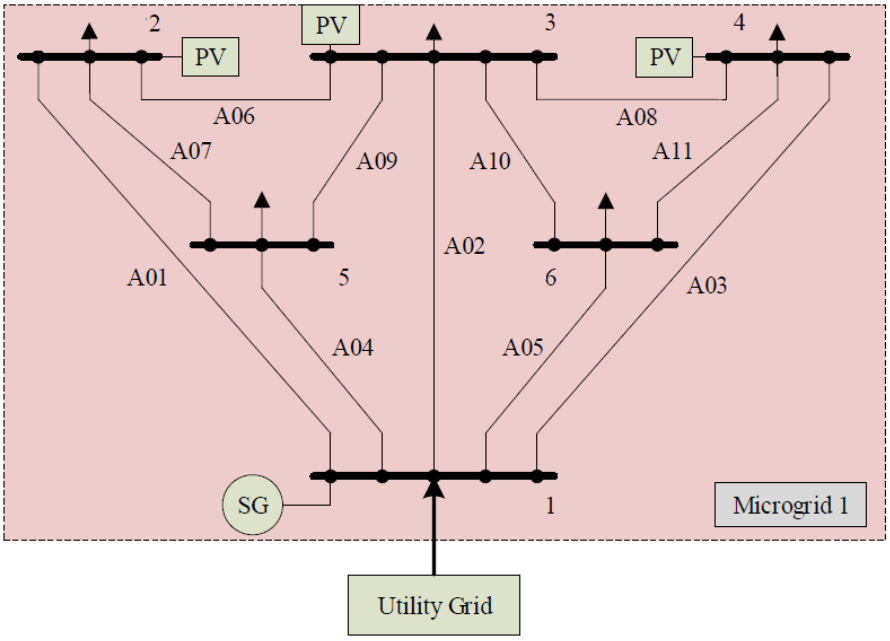

Figure 2. Benchmark microgrid, adapted from (23)

Batteries are not shown in Figure 1, but are installed in buses 2, 3 and 4. The main resources installed in MG1 can be seen in Table 2.

Table 2. Benchmark microgrid data, adapted from (23)

	Resources				
Bus	**Max PV power (pu)**	**Max Thermal Power (pu)**	**BESS capacity (pu.h)**	**BESS max charge and discharge power (pu)**	**Peak Load (pu.h)**
1	-	0.5	-	-	-
2	0.2	-	0.3	0.2	0.2125
3	0.24	-	0.4	0.24	0.3329
4	0.2	-	0.3	0.2	0.205
5	-	-	-	-	0.1257
6	-	-	-	-	0.1056

The work in (23) provides real-world data for PV generation and non-controllable loads for one year (364 days). These samples were separated by the year season since PV generation will be highly affected by seasonal changes, which resulted in 91 real-world scenarios for each season of the year. The summer season was considered for this work.

To expand the size of this set, an oversampling process was conducted by adding and subtracting random small deltas to historical data scenarios, generating new synthetic scenarios that are not real-world data, but would be in the realm of possibilities for the historical data.

Therefore, the final set of uncertainty consisted of 910 scenarios, being 91 real-world scenarios from (23) (which represent the summer season of one year), plus 9 more summers of synthetic data created based on the real-world data.

RESULTS

The microgrid was simulated using the DDRO approach and using a traditional adaptive robust optimization (ARO) approach for comparison. For the ARO simulation, a 15% uncertainty budget was considered for both PV generation and non-controllable loads, meaning that the overall amount of PV generation and non-controllable load can vary by up to 15% from the base case, while for DDRO the historic set constructed in the previous section was used to bound the uncertainty set. The detailed C&CG iterative process is shown for DDRO below.

In the first stage of the first iteration (which has no uncertainty and considers the base case), the dispatch of DERs in MG can be seen in Figure 3.

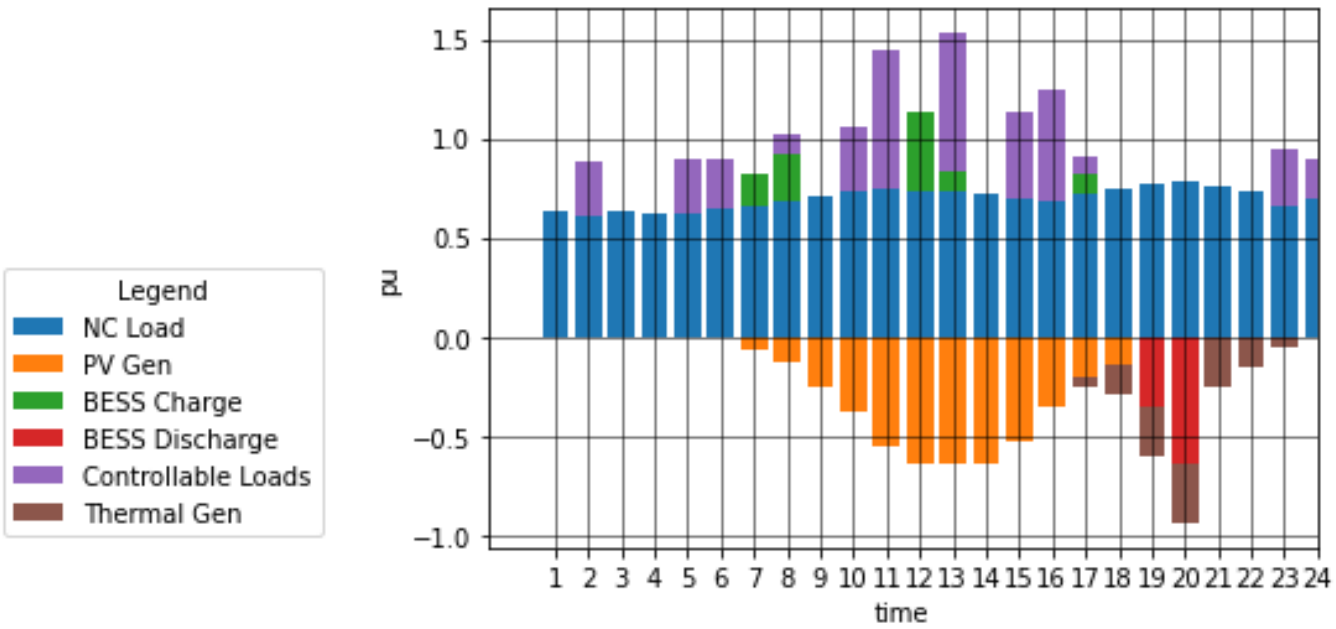

Figure 3. First stage, k = 1

As can be seen, the battery was charged off-peak and discharged in peak tariff periods, and the thermal generator was ramped-up a few periods before the 6PM start of the peak tariff period to be operated at full capacity during this expensive energy period. Controllable loads were allocated fully outside of the peak time. The operational cost for the MG in this scenario was $ 124,600.60, and so LB = 124,600,60.

Following with the algorithm, BESS, CL, and the thermal generator variables were fixed in the second stage, and the worst-case scenario for PV and NCL was searched, resulting in Figure 4.

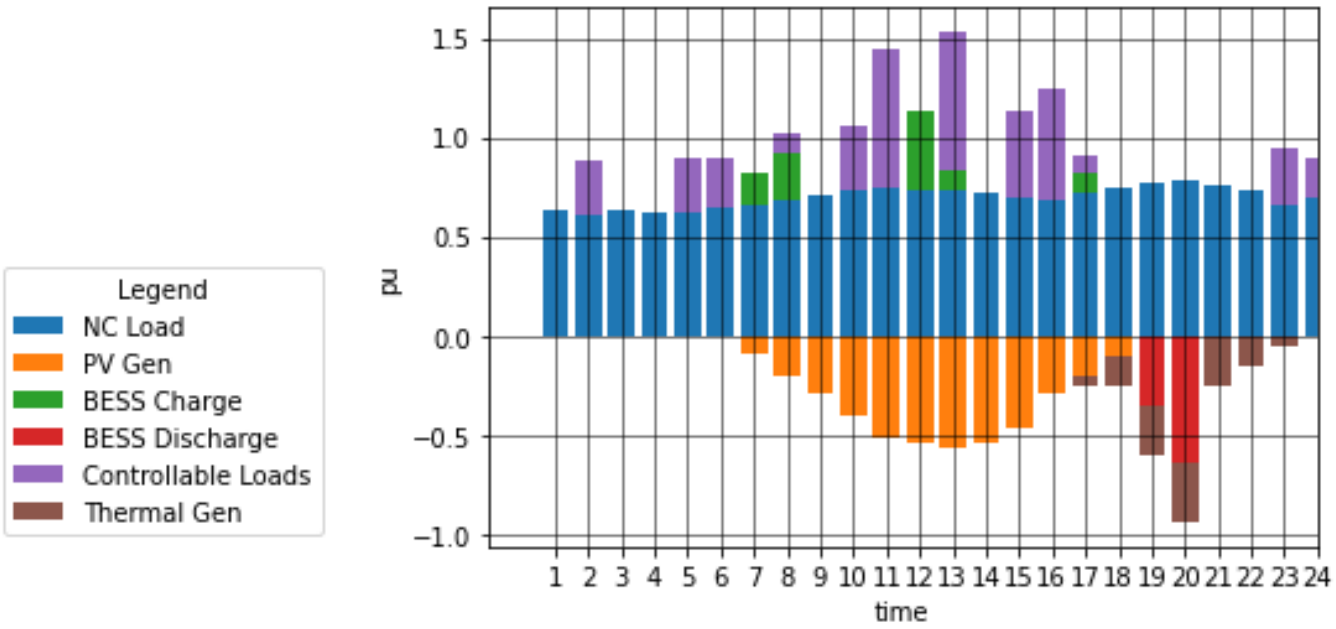

Figure 4. Second stage, k = 1

In this stage, it is possible to observe a decrease in PV generation, meaning that the solver found a worst feasible scenario of PV for the operating conditions found in the first stage. Operational costs in this stage rose to $ 126,934.81, and so UB = 126,934.81.

Since UB-LB is greater than the tolerance, the uncertainty scenario generated in the second stage is incorporated in the first stage, and a new iteration begins. The dispatch of DERs for the second stage can be seen in Figure 5.

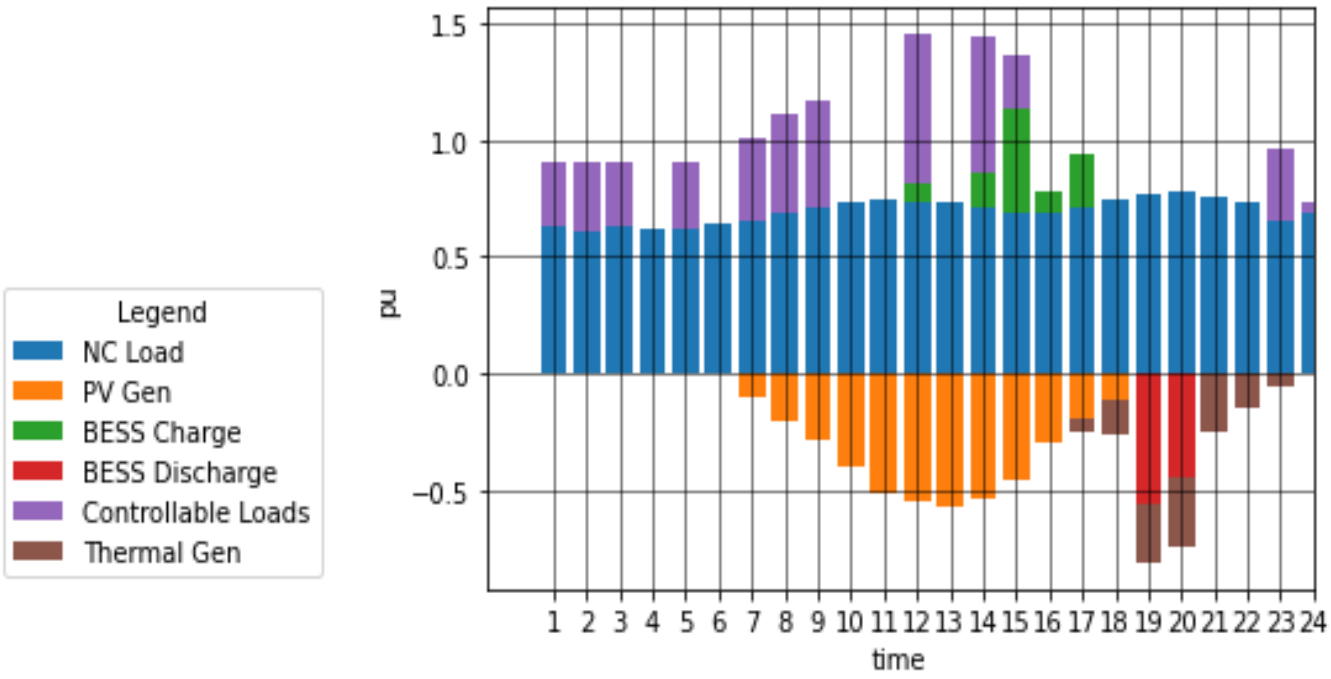

Figure 5. First stage, k = 2

Comparing Figure 5 with Figure 3 shows that the operation of CL and BESS was slightly changed from the first stage of the first iteration. The obtained cost for this stage was $ 126,934.81, so the new LB is 126,934.81. This change means that the first stage could not find a better solution for the new uncertainty scenario. So, the second stage is performed, and if it cannot find a worse uncertainty realization, the process would reach convergence. The dispatch for the second stage can be seen in Figure 6.

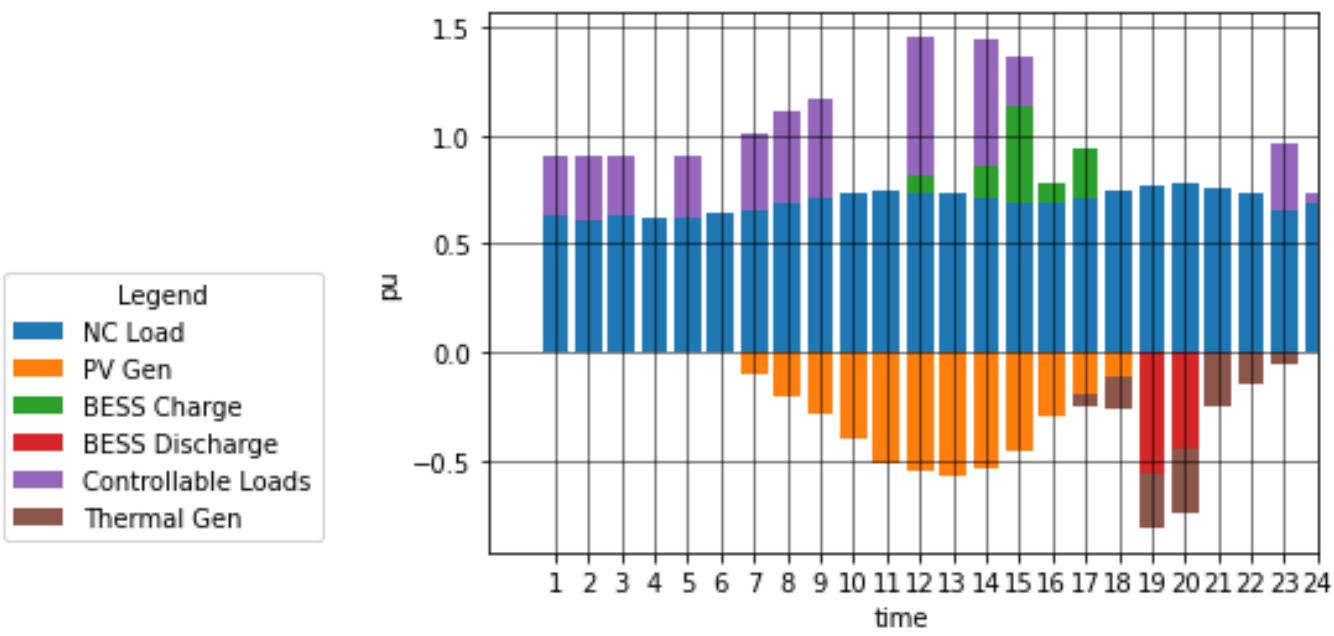

Figure 6. Second stage, k = 2

The cost obtained was $ 126,934.81, and so UB = 126,934.81. In this case, convergence was achieved in 2 iterations and the total computational time was 8.85 seconds.

Comparing Figure 6 and Figure 4, the presence of uncertainties caused changes in the operational decisions, mainly regarding BESS and demand response, showing the importance of uncertainty consideration for better planning. Also, the solution is immune to the worst-case scenario and therefore to all other uncertainty scenarios that represent better operational conditions.

Table 3 shows the costs comparison considering the base case (without uncertainties), the ARO scenario and the DDRO approach.

Table 3. Operational costs, different optimization approaches

Base Case	DDRO, summer	ARO, $\Gamma = 15\%$
124,600.60	126,934.54 (+1.8%)	165,137.18 (+32,5%)

In ARO, the historical data for the uncertain variables is unknown, so an arbitrary uncertainty budget is established. Using a 15% uncertainty budget for both PV generation and uncontrollable loads, the final operational cost obtained was $ 165,137.18. That represents an increase of 32.5% from the base case with no uncertainties, compared to a mere 1.8% increase when the uncertainty set was bounded using DDRO, showing the advantages of using the historical data to create a more realistic uncertainty set.

In terms of grid transactions, Figure 7 shows the amount of energy exchanged with the upstream grid for the DDRO approach.

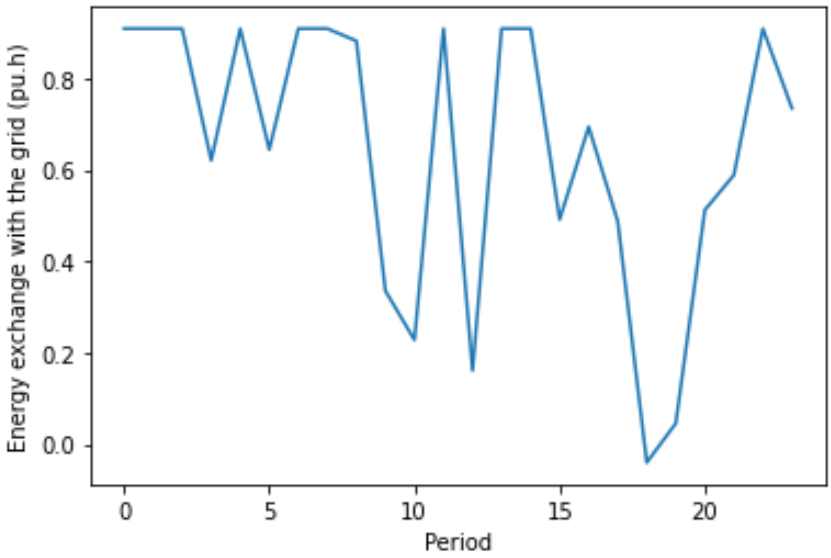

Figure 7. Energy exchange with the upstream grid

The load factor constraints contained the energy exchanges with the grid to a moderate value, without peaks from a large allocation of controllable loads, for example. The exchange is lower during the afternoon because of the peak PV generation (less energy is necessary from the grid) and the lowest in the peak tariff period because batteries and the thermal generators are utilized at their full capacity to avoid paying expensive tariffs to the DSO.

CONCLUSIONS

The objective of this work was to develop a comprehensive linear model for the day-ahead optimization of microgrids, using a novel data-driven robust optimization approach (DDRO) that was not previously used for MG systems. A MILP model was proposed and a tri-level min-max-min formulation was created. The formulation was solved using a two-stage decomposition and the column and constraint generation algorithm (C&CG).

The results highlight the importance of considering uncertainties when planning the operational decisions of MG systems, since the uncertainties can modify the ideal utilization of the distributed energy resources through the day. Also, while in the DDRO scenario the costs rose by only 1.8% when compared to the base case without uncertainties, showing that the random historic scenario that was chosen was already close to the worst-case scenario in terms of cost, other more optimistic scenarios could have been chosen, which would cause a lower operational cost for the base case and therefore a higher percentual increase when uncertainties are considered.

Also, by finding and optimizing for the worst-case scenario of uncertainties, the DDRO solution ($ 126,934,54) is immune regarding costs to the uncertainty set that was considered. This means that the DDRO model will present equal or lower overall operational costs for all other uncertainty scenarios in the uncertainty set.

It is also highlighted the importance of demand response in providing flexibility for the MG operation and allowing load factor constraints to be applied without convergence issues.

Finally, the fast-converging time for simulation is highlighted, showing that DDRO is a capable tool for finding historically accurate results without the high computational burden found in other optimization techniques such as stochastic programming.

Acknowledgments This research was funded by the Companhia Paranaense de Energia – COPEL research and technological development (RTD) program, through the PD-02866-0511/2019 project, regulated by ANEEL. The authors thank the support of CAPES – Brazilian Agency for Support and Evaluation of Graduate Education within the Ministry of Education of Brazil. We also thank the CAPES-PRINT-UFPR Project – Finance Code 001.

REFERENCES

1. Tenfen D, Finardi EC. A mixed integer linear programming model for the energy management problem of microgrids. Electric Power Systems Research [Internet]. 2015; Available from: https://www.sciencedirect.com/science/article/pii/S0378779614004659
2. Umeozor EC, Trifkovic M. Operational scheduling of microgrids via parametric programming. Appl Energy [Internet]. 2016; Available from: https://www.sciencedirect.com/science/article/pii/S0306261916310960
3. Nwulu NI, Xia X. Optimal dispatch for a microgrid incorporating renewables and demand response. Renew Energy [Internet]. 2017; Available from: https://www.sciencedirect.com/science/article/pii/S0960148116307273
4. Aliasghari P, Mohammadi-Ivatloo B, Alipour M, Optimal scheduling of plug-in electric vehicles and renewable micro-grid in energy and reserve markets considering demand response program. J Clean Prod [Internet]. 2018; Available from: https://www.sciencedirect.com/science/article/pii/S0959652618307157
5. Guo Y, Zhao C. Islanding-aware robust energy management for microgrids. IEEE Trans Smart Grid. 2018;9(2):1301–9.
6. Mehdizadeh A, Taghizadegan N, Salehi J. Risk-based energy management of renewable-based microgrid using information gap decision theory in the presence of peak load management. Appl Energy [Internet]. 2018; Available from: https://www.sciencedirect.com/science/article/pii/S0306261917316835
7. Moretti L, Martelli E, Manzolini G. An efficient robust optimization model for the unit commitment and dispatch of multi-energy systems and microgrids. Appl Energy [Internet]. 2020; Available from: https://www.sciencedirect.com/science/article/pii/S0306261919315466
8. Zhang J, Wu Y, Guo Y, Wang B, Wang H, Liu H. A hybrid harmony search algorithm with differential evolution for day-ahead scheduling problem of a microgrid with consideration of power flow constraints. Appl Energy [Internet]. 2016; Available from: https://www.sciencedirect.com/science/article/pii/S030626191631337X
9. Monfared HJ, Ghasemi A, Loni A, Marzband M. A hybrid price-based demand response program for the residential micro-grid. Energy [Internet]. 2019; Available from: https://www.sciencedirect.com/science/article/pii/S0360544219313726
10. Zia MF, Elbouchikhi E, Benbouzid M. Optimal operational planning of scalable DC microgrid with demand response, islanding, and battery degradation cost considerations. Appl Energy [Internet]. 2019; Available from: https://www.sciencedirect.com/science/article/pii/S0306261919300406
11. Liu G, Starke M, Zhang X. A MILP-based distribution optimal power flow model for microgrid operation. Power and Energy Society. [Internet]. 2016; Available from: https://ieeexplore.ieee.org/abstract/document/7741704/
12. Mortaz E, Valenzuela J. Microgrid energy scheduling using storage from electric vehicles. Electr Pow Syst Res [Internet]. 2017; Available from: https://www.sciencedirect.com/science/article/pii/S0378779616304692
13. Ebrahimi MR, Amjady N. Adaptive robust optimization framework for day-ahead microgrid scheduling. Int. J. Electr. Power and Energy Syst. [Internet]. 2019;107(February 2018):213–23. Available from: https://doi.org/10.1016/j.ijepes.2018.11.029
14. Wang B, Zhang C, Dong Z. Interval Optimization Based Coordination of Demand Response and Battery Energy Storage System Considering SoC Management in A Microgrid. IEEE Trans Sustain Energy [Internet]. 2020; Available from: https://ieeexplore.ieee.org/abstract/document/9043605/
15. Velloso A, Street A, Pozo D, Arroyo JM, Cobos NG. Two-stage robust unit commitment for co-optimized electricity markets: An adaptive data-driven approach for scenario-based uncertainty sets. IEEE Trans Sustain Energy. 2020;11(2):958–69.
16. Wang L, Jiang C, Gong K, Si R, Shao H, Liu W. Data-driven distributionally robust economic dispatch for distribution network with multiple microgrids. IET Generation, Transmission and Distribution. 2020;14(24):5816–22.
17. Delfino F, Ferro G, Robba M. An Energy Management Platform for the Optimal Control of Active and Reactive Powers in Sustainable Microgrids. IEEE Trans Ind Appl [Internet]. 2019; Available from: https://ieeexplore.ieee.org/abstract/document/8700197/

18. Kim TH, Shin H, Kwag K, Kim W. A parallel multi-period optimal scheduling algorithm in microgrids with energy storage systems using decomposed inter-temporal constraints. Energy [Internet]. 2020; Available from: https://www.sciencedirect.com/science/article/pii/S0360544220307763
19. Jin M, Feng W, Liu P, Marnay C, Spanos C. MOD-DR: Microgrid optimal dispatch with demand response. Appl Energy [Internet]. 2017; Available from: https://www.sciencedirect.com/science/article/pii/S030626191631724X
20. Xu B, Oudalov A, Ulbig A, Andersson G, Kirschen DS. Modeling of lithium-ion battery degradation for cell life assessment. IEEE Trans Smart Grid. 2018;9(2):1131–40.
21. Arroyo JM, Conejo AJ. Modeling of start-up and shut-down power trajectories of thermal units. IEEE Trans. Power Syst. 2004;19(3):1562–8.
22. Yuan H, Li F, Wei Y, Zhu J. Novel Linearized Power Flow and Linearized OPF Models for Active Distribution Networks With Application in Distribution LMP. IEEE Trans Smart Grid. 2018;
23. Alam MN, Chakrabarti S, Liang X. A Benchmark Test System for Networked Microgrids. IEEE Trans Industr Inform. 2020;16(10):6217–30.